JOURNAL OF MATERIALS SCIENCE 25 (1990) 1957–1964

Interaction between titanium and SiC

S. K. CHOI, M. CHANDRASEKARAN, M. J. BRABERS
Department of Metallurgy and Materials Engineering, Katholieke Universiteit Leuven, de Croylaan 2, B-3030 Leuven, Belgium

Interaction between titanium and SiC particles was studied by electron microprobe, scanning electron microscopy (SEM) and transmission electron microscopy (TEM). The distribution of the reaction products from the SiC to the titanium end is reported. Particular attention is given to the microstructure and phase analysis in areas near to the SiC. The implications of the observed microstructural and structural details are discussed.

1. Introduction

There are many potential applications for high quality, low density titanium composites in advanced engineering components. In particular, the Ti–SiC system finds use not only as a composite material but also in the joining of ceramics and metals. While chemical interfacial reaction limits the interfacial stability in the former case, it provides good bonding effects for the latter application. The reaction layer and the interdiffusion in Ti–SiC have been extensively studied [1–11]. Silicon carbide filaments [1–4], silicon carbide coated boron filaments [5–8], and silicon carbide cylinders or pellets [9] have been employed in these investigations. It is now generally accepted that the interdiffusion of silicon, carbon and titanium (across the interface) results in the formation of Ti_5Si_3 and TiC [10, 11]. Nevertheless, the formation of certain ternary reaction products and the reaction mechanism is still subject to discussion. In particular, the formation of a compound, Ti_3SiC_2, has been claimed by Martineau *et al.* [1] in a stoichiometric SiC filament/titanium matrix, by Ratliff and Powell [9] in SiC/Ti diffusion couples, and by Morozumi *et al.* [12] in SiC/Ti/SiC diffusion couples. On the other hand, several other investigators working with fibrous samples [2, 3], titanium alloy/SiC composites [3], and W–SiC/Ti composites [7] did not find this ternary compound.

On the reaction mechanism, Ratliff and Powell [9] have proposed the simultaneous formation of $Ti_5Si_3(C)$ and TiC_{1-x} with the latter phase near to SiC. These authors have further suggested that when the TiC adjacent to the filament surface becomes sufficiently supersaturated with respect to both silicon and carbon, the ternary phase Ti_3SiC_2 is formed. On the other hand, Martineau *et al.* [1] have proposed an almost opposite scheme where as a first step Ti_3SiC_2 and $Ti_5Si_3C_x$ supposedly form simultaneously. The authors also suggest that later, as the $Ti_5Si_3(C)$ sublayer grows and becomes sufficiently supersaturated with respect to carbon, TiC precipitates in a silicide matrix. Contrary to the conclusion of Ratliff and Powell [9], the inner side of the binary sublayer has been claimed by Martineau *et al.* [1] to be preferentially made of $Ti_5Si_3(C)$.

In view of the above controversy, the present authors have earlier conducted a study of the reaction layer between titanium and SiC as part of an attempt to assess the reaction between SiC and some transition metals [13]. The binary zone of TiC and Ti_5Si_3, and the thin layer separating SiC and this binary zone after 900° C heat treatment, have been confirmed in that study. The binary zone was formed by the diffusion of silicon and carbon into metal, and the thin layer was formed by the diffusion of titanium into SiC. The thin layer adjoining SiC presented too small a volume to be analysed by X-ray diffraction (XRD) while the minimum probe size and beam spreading in the electron-probe micro-analyser (EPMA) prevented a proper analysis of this same thin layer. In the present work, an attempt has been made to investigate the thin layer and binary zone in samples reacted for short as well as long time by TEM and diffraction. The results of this investigation are reported, and the microstructural evolution discussed in terms of diffusion of titanium, silicon and carbon.

2. Experimental procedures

The starting SiC contained 1.5 wt % total impurities (principal impurities were SiO_2 and carbon). The starting composition of titanium was as follows: Ti(Fe < 0.1; Si < 0.05) H_2 < 0.1; N_2 < 0.05; O_2 < 0.5 wt %). The oxygen content of titanium is uncertain. After mixing the ceramic and metal powder in a volume ratio of 3 : 7 (ceramic : metal), the specimens were pelleted by hydraulic pressing at 45 MPa. The pellets were then heated in the range of 600 to 1300° C for 5 to 100 h in a 5 ml sec^{-1} argon gas flow (99.99% argon, 10 p.p.m. O_2 and 80 p.p.m. N_2) and finally cooled in the same atmosphere.

Any surface oxide remaining after the treatment was removed by grinding. Either the flat surface after such grinding or powder obtained by crushing such pellets were used for XRD analysis. Pellets were embedded under vacuum in epofix resin. The embedded samples were then ground and finally polished in 1 μm diamond paste. These polished samples were used for microstructural and microchemical analytical studies, which were performed by SEM and EPMA.

EPMA of the samples was carried out in a JEOL

0022–2461/90 $03.00 + .12

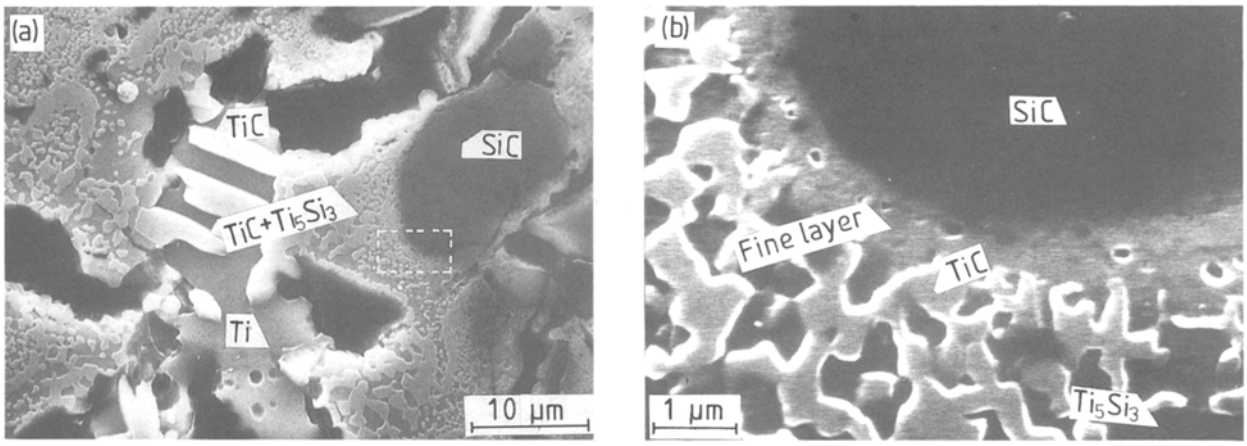

Figure 1 SEM photograph of Ti/SiC, 100 h at 900° C, etched. (a) × 2000, (b) × 14000.

733 unit. For the analysis of elements with an atomic number above 11 (Na), energy dispersive spectroscopy (EDS) was used; carbide and oxide were analysed by wavelength dispersive spectroscopy (WDS). In the EDS mode a 20 kV operating voltage and 10^{-8} ampere beam current were employed, whereas in the WDS mode the operating voltage was reduced to 10 kV and the beam current increased to 10^{-6} amperes.

Samples for TEM observation were prepared by cutting out 3 mm diameter discs from the bulk material which were later ground to 30 μm thickness and finally ion milled with 5 kV argon ions to obtain electron-transparent regions. The samples were examined in a JEOL 200 CX microscope operated at 200 kV.

3. Results

3.1. Diffusion layer analysis by SEM and EPMA

Some of our SEM and EPMA microstructural analysis has been presented earlier [13], but are given again here to develop the structural basis for the TEM analysis.

The reaction products could be distinguished after etching and, as seen in Fig. 1, a 10 to 15 μm-thick interaction layer was obtained after treatment for 100 h at 900° C. The reaction layer was made up of three sublayers: a very fine layer near SiC, Fig. 1b, a mixture of TiC and Ti_5Si_3, and TiC crystals towards the titanium side. Microchemical analysis of this reaction layer was performed by EPMA. The X-ray line analysis (Fig. 2b) for CK_α and SiK_α, and the point analysis (Fig. 2c) for SiK_α and TiK_α indicated the differences in level of carbon and silicon between the bright and dark-grey phases. This analysis showed that the preferentially etched dark-grey matrix phase is Ti_5Si_3 while the bright phase is TiC.

Spots (initially assumed to be holes) in a regular array surrounding the SiC were observed in specimens treated at 900° C. These features were not found in specimens treated at lower temperatures. Figure 3 demonstrates that the layer between SiC and these features grows as the time increases from 5 to 100 h. The analysis of this layer adjacent to SiC was made difficult by the probe size and the beam spreading in EPMA, and the small volume to be analysed by XRD. The X-ray line analysis in Fig. 4 shows the existence of titanium, carbon and silicon in this layer which qualitatively is not enough to identify it as a ternary compound. It is interesting to note the high intensity of SiK_α around these spots or features in the X-ray line analysis of the layer.

3.2. Analysis by TEM

The SiC was either 6H or 4H type, with the former

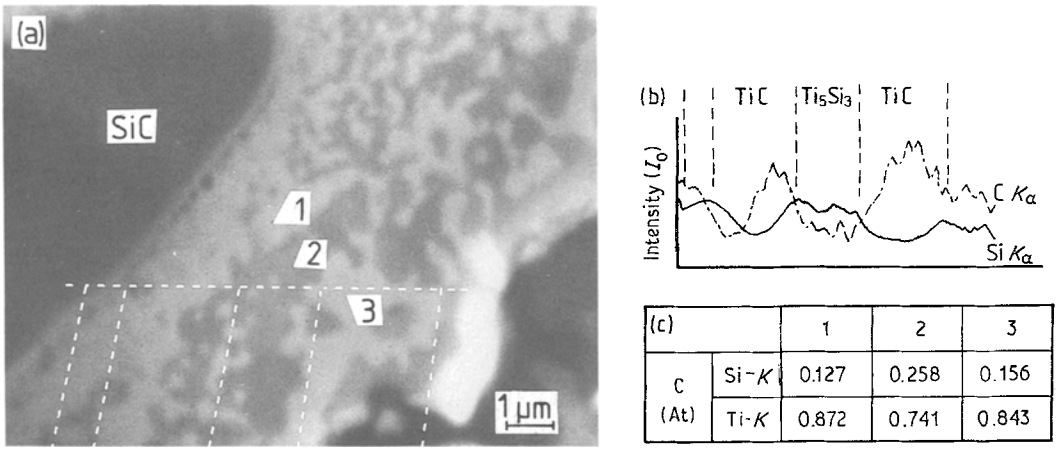

(c)		1	2	3
C (At)	Si-K	0.127	0.258	0.156
	Ti-K	0.872	0.741	0.843

Figure 2 Microchemical analysis of reaction layer. (a) SEM photograph (× 7800); (b) X-ray line analysis of SiK_α, CK_α; (c) semi-quantitative analysis of SiK_α, TiK_α.

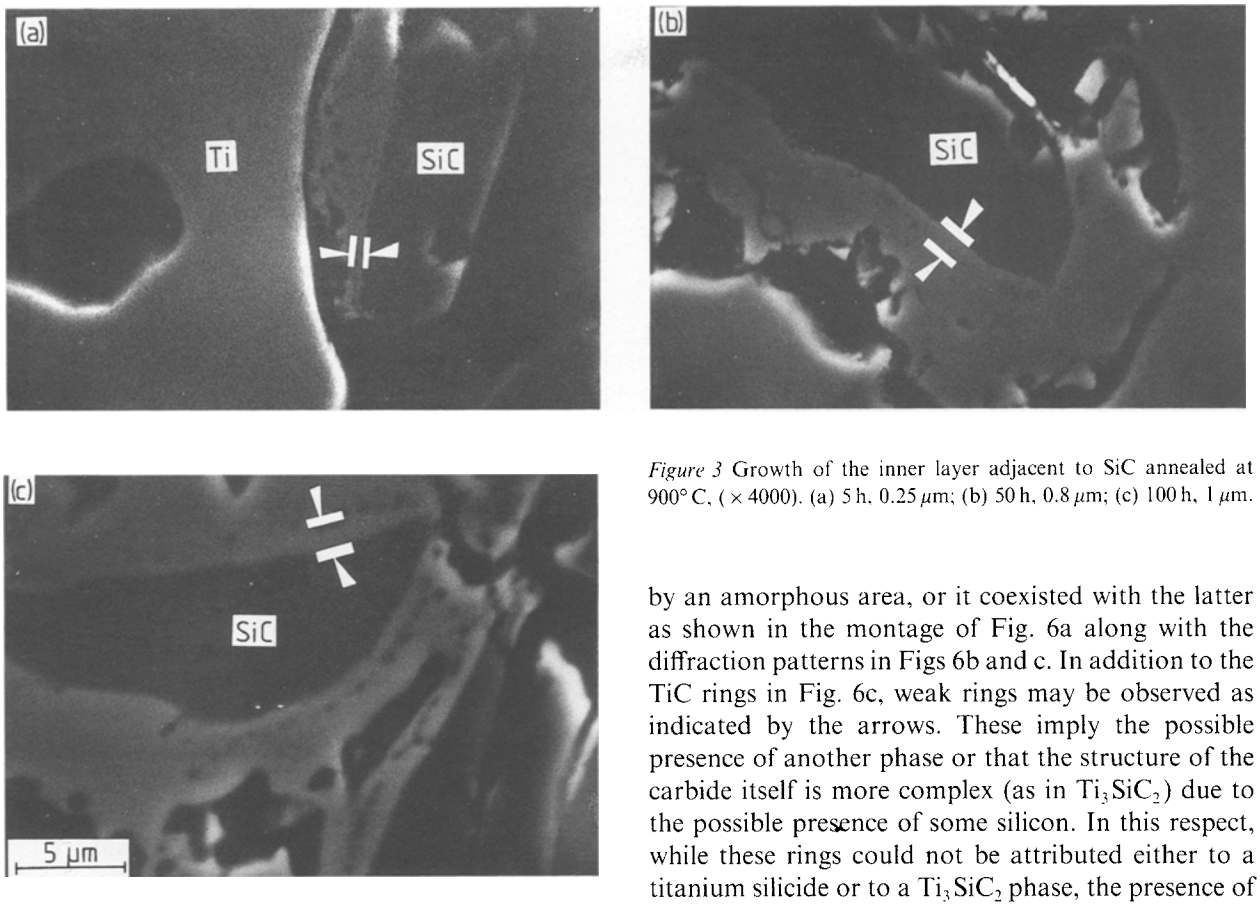

Figure 3 Growth of the inner layer adjacent to SiC annealed at 900° C, (× 4000). (a) 5 h, 0.25 μm; (b) 50 h, 0.8 μm; (c) 100 h, 1 μm.

predominant. The reaction between SiC and titanium to be described below was, however, independent of the type of SiC.

In samples after short reaction times, 900° C for 5 h, the available thin area did not permit simultaneous observation of SiC, titanium and the reaction zone. Information regarding the reaction was, therefore, gathered from observing areas near SiC. Generally, a very fine-grained TiC zone was encountered near the SiC. This was confirmed by electron diffraction patterns such as the one shown in Fig. 5. Even though intensities in electron diffraction may be affected by dynamical effects, it is interesting to note in this figure that the {1 1 1} ring is much weaker, more than predicted under kinematical conditions, than the {2 0 0} ring. The TiC area was often separated from the SiC by an amorphous area, or it coexisted with the latter as shown in the montage of Fig. 6a along with the diffraction patterns in Figs 6b and c. In addition to the TiC rings in Fig. 6c, weak rings may be observed as indicated by the arrows. These imply the possible presence of another phase or that the structure of the carbide itself is more complex (as in Ti_3SiC_2) due to the possible presence of some silicon. In this respect, while these rings could not be attributed either to a titanium silicide or to a Ti_3SiC_2 phase, the presence of such a phase close to the SiC was evidenced in the diffraction patterns and microstructure from other areas of the same sample (Fig. 7) or in samples reacted for a longer time (Fig. 8). The semi-continuous rings due to the fine TiC crystals are apparent in these diffraction patterns (Figs 7 and 8). The reflections that lie within the innermost ring and in the region separating the rings could be attributed to Ti_5Si_3. Bright-field (Figs 7 and 8a) and dark-field (Fig. 7b) micrographs obtained using such reflections show the distribution of these relatively large Ti_5Si_3 crystals. Thus, the reaction zone near SiC is made up of TiC, Ti_5Si_3, and Ti_3SiC_2 phases the last being present in the least significant amounts. The TiC phase is considered to be the dominant one, as evidenced from the diffraction patterns (Figs 7c and 8c), as well as being the phase in contact with SiC. As proof of the latter aspect, a

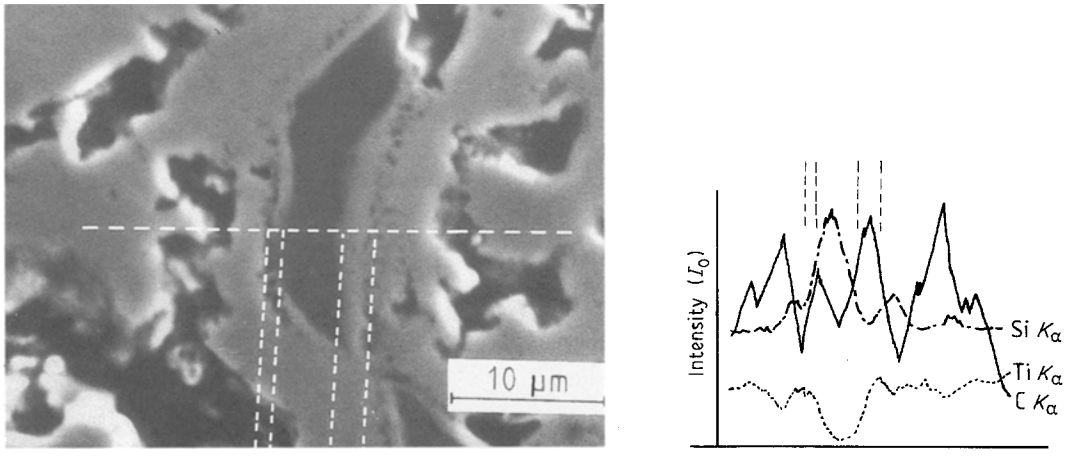

Figure 4 X-ray line analysis of SiK_α, TiK_α, CK_α for inner layer after 900° C, 100 h.

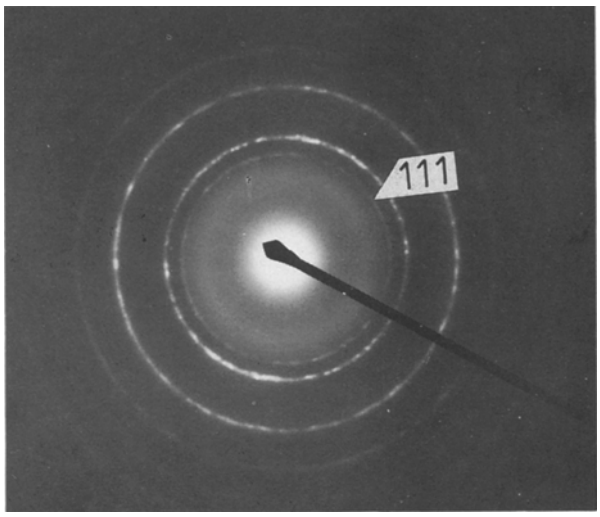

Figure 5 Electron diffraction patterns of a very fine-grained TiC zone adjoining SiC.

obtained using such reflections show the distribution of these relatively large Ti_5Si_3 crystals. Thus, the reaction zone near SiC is made up of TiC, Ti_5Si_3, and Ti_3SiC_2 phases the last being present in the least signifi- microdiffraction pattern (Fig. 9b) from a small grain adjoining SiC in Fig. 9a is presented which can be consistently indexed as a $\langle 1\,1\,1 \rangle$ zone axis pattern from TiC.

In the more reacted samples, (900° C for 100 h), larger grains of Ti_5Si_3 were found just behind the TiC layer in contact with SiC. The presence of such Ti_5Si_3 grains was confirmed by tilting experiments to obtain single crystal spot patterns which could be uniquely indexed as from Ti_5Si_3. An example of the Ti_5Si_3 microstructure and the corresponding diffraction are shown in Figs 10a and b.

Progressively larger grains of both TiC and Ti_5Si_3 were encountered approaching the titanium end. A montage revealing this gradation in grain size is shown in Fig. 11. The larger grains of TiC and Ti_5Si_3 could be identified from their single-crystal spot pattern (Figs 11b and c, respectively). These phases could also be distinguished from the image contrast in the bright field images. TiC exhibited a mottled contrast (Fig. 12) which could be readily distinguished from the rather featureless grains of Ti_5Si_3. Such a contrast difference probably resulted from the different milling behaviour of the two phases when bombarded by argon ions during sample preparation. Some carbide grains exhibited additional reflections, in the diffraction patterns, at one half distances of the fcc TiC reflections. This was, however, observed only in the case of reflections with $h + k + l = 2n + 1$ (Figs 13a and b) and not in the case of reflections where $h + k + l = 2n$ (Figs 11b and 13c).

It was also noted generally that the phase in contact with titanium was Ti_5Si_3 and not TiC. An example of this observation is given in Fig. 14 where the Ti_5Si_3 phase may be distinguished easily from the TiC phase by the contrast difference mentioned above.

4. Discussion

The results of the present investigation suggest that the thin layer adjoining SiC is made up of fine-grained TiC and Ti_5Si_3. Of these two, the majority-phase TiC has been observed to be the phase in contact with SiC. These observations support Ratliff and Powell's findings [9] rather than those of Martineau *et al.* [1] on the issue of the phase in contact with SiC. Nevertheless, the intensity differences observed in the diffraction patterns between the $\{1\,1\,1\}$ and $\{2\,0\,0\}$ rings of this fcc carbide could imply the presence of some impurities, notably silicon. The phase may thus be more aptly designated as TiC(Si). Further, diffraction evidence also suggests the presence, though occasionally, of Ti_3SiC_2 in the thin layer.

On the basis of the above results, the mechanism

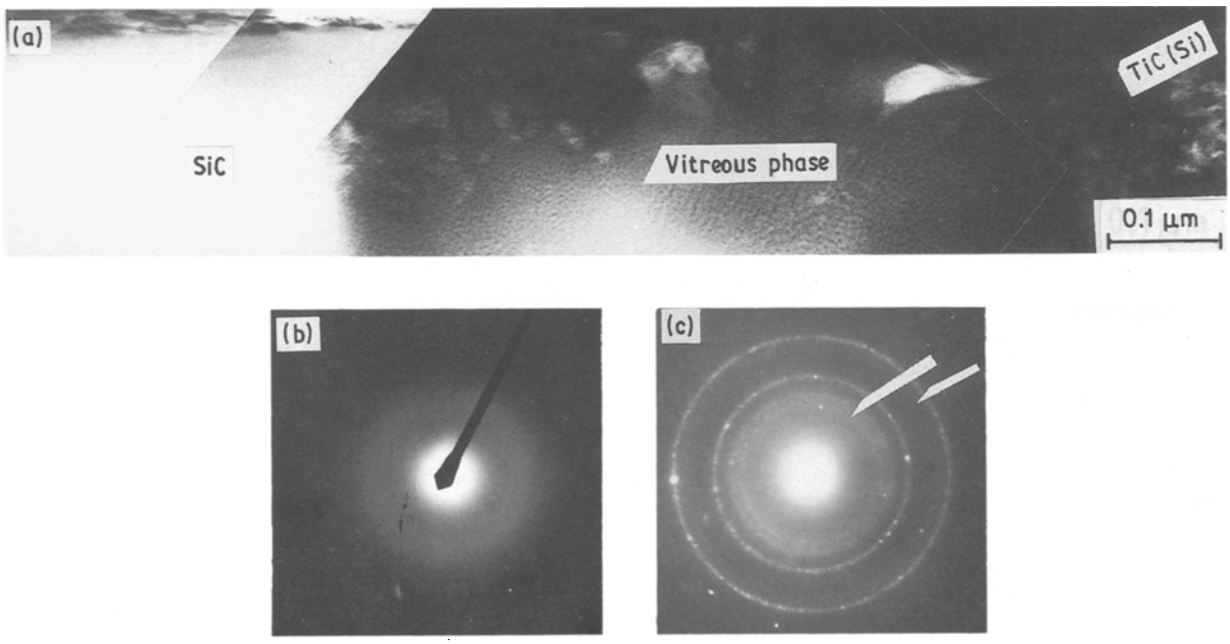

Figure 6 After 900° C, 5 h. (a) Montage of TiC area separated from the SiC by an amorphous area and diffraction pattern of (b) amorphous area and (c) TiC zone, weak rings not pertaining to fcc TiC indicated by arrows.

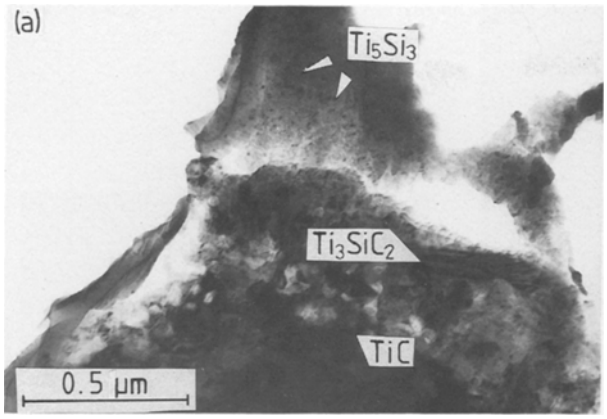

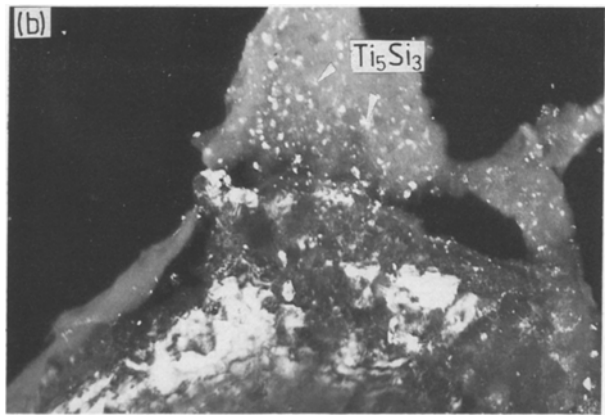

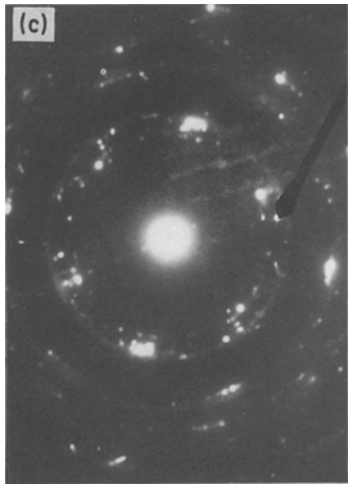

Figure 7 After 900° C, 5 h. (a) Bright-field; (b) dark-field micrograph, and (c) diffraction pattern.

for the thin layer which separates SiC and the metal-reaction zone can be proposed as follows. The thin layer which is actually formed by titanium diffusion into SiC is made up primarily of fine-grained TiC. It confirms the higher stability of TiC over that of Ti_5Si_3. Subsequently, diffusion of silicon and carbon through the thin layer can give rise to growth of Ti_5Si_3 and the occasionally present Ti_3SiC_2. The mechanism for the layer which is formed by silicon and carbon into titanium can be described as follows. In the first step, TiC can form near SiC followed by the diffusion of silicon and carbon through this layer. In the second step, Ti_5Si_3 precipitates grow rapidly by taking up the neighbouring TiC. Finally, the surplus amount of carbon forms TiC crystals at the edge of the metal reaction zone. These mechanisms are indicated on a reaction of the ternary phase diagram proposed by Brukl [14] in Fig. 15. The dotted lines represent a diffusion path of silicon and carbon into metal or of metal into SiC. It is assumed that the diffusion path of silicon and carbon into metal follows the field of $Ti_5Si_3(C)$–TiC_{1-x}–β-Ti. The diffusion path of titanium into SiC follows the field of SiC–T–TiC_{1-x}. The higher stability of TiC leads the path into the field SiC–T–TiC_{1-x} rather than $TiSi_2$–SiC–T. The absence of $TiSi_2$ can be explained by this assumption.

The near-regular array of spots surrounding the SiC observed in SEM on specimens treated at 900° C gives the physical appearance of holes due to a possible Kirkendall effect [15]. The large difference in the diffusion rate of titanium into SiC and silicon and carbon into titanium [9] could indeed support such a premise. However, microanalysis (Fig. 4b) around such spots indicated a rather high silicon content. In addition, no convincing evidence of such holes were found in TEM observations which instead indicated the presence of rather large grains of Ti_5Si_3 adjacent to the fine-grained TiC(Si) layer. Since these silicides could as well explain the high silicon content in the microanalysis, the interpretation of the spots as Kirkendall pores and its possible implications have to be held in abeyance until affirmative TEM evidence is obtained.

The presence of an amorphous layer coexisting with or separating the TiC from the SiC was mentioned

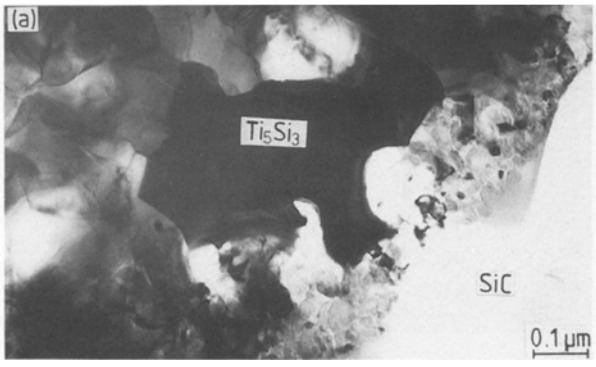

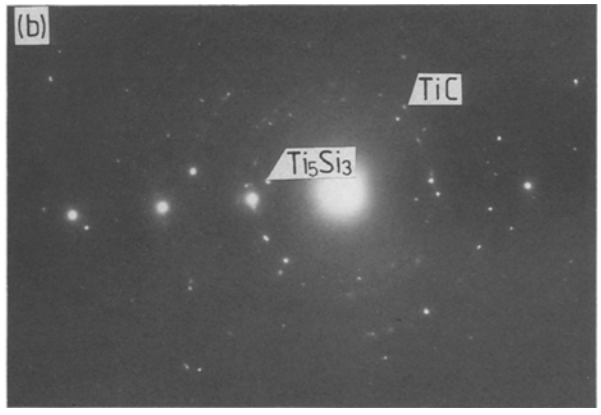

Figure 8 Reacted for a longer time 900° C, 100 h. (a) Bright-field micrograph; (b) diffraction pattern.

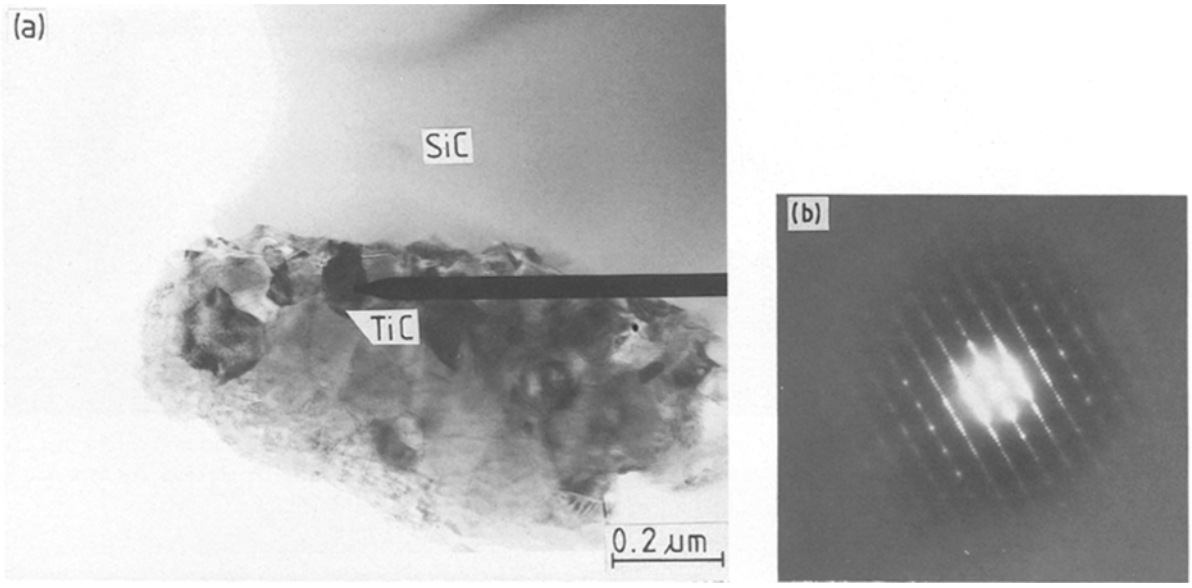

Figure 9 After 900°, 100 h. (a) Reaction layer adjoining SiC; (b) microdiffraction pattern of small grain of TiC [1 1 1] zone axis along with SiC reflections.

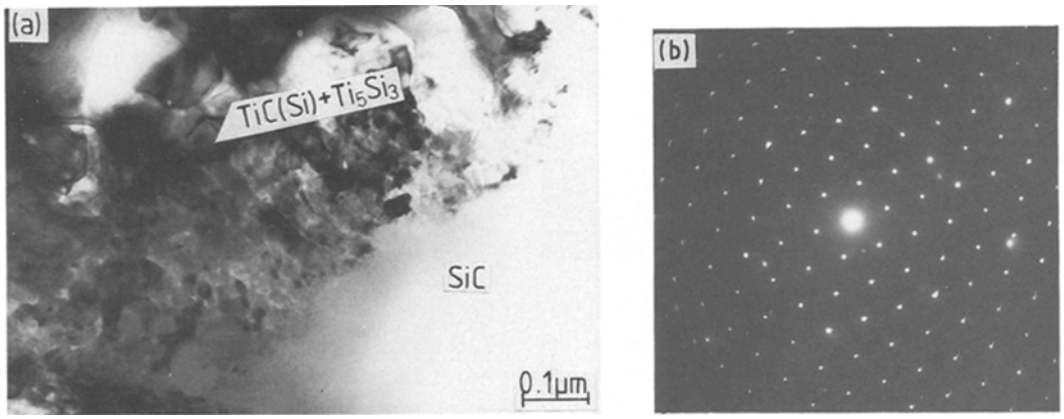

Figure 10 After 900° C, 100 h. (a) Microstructure of Ti_5Si_3 adjacent to TiC crystals; (b) [0 0 0 1] zone axis pattern from Ti_5Si_3.

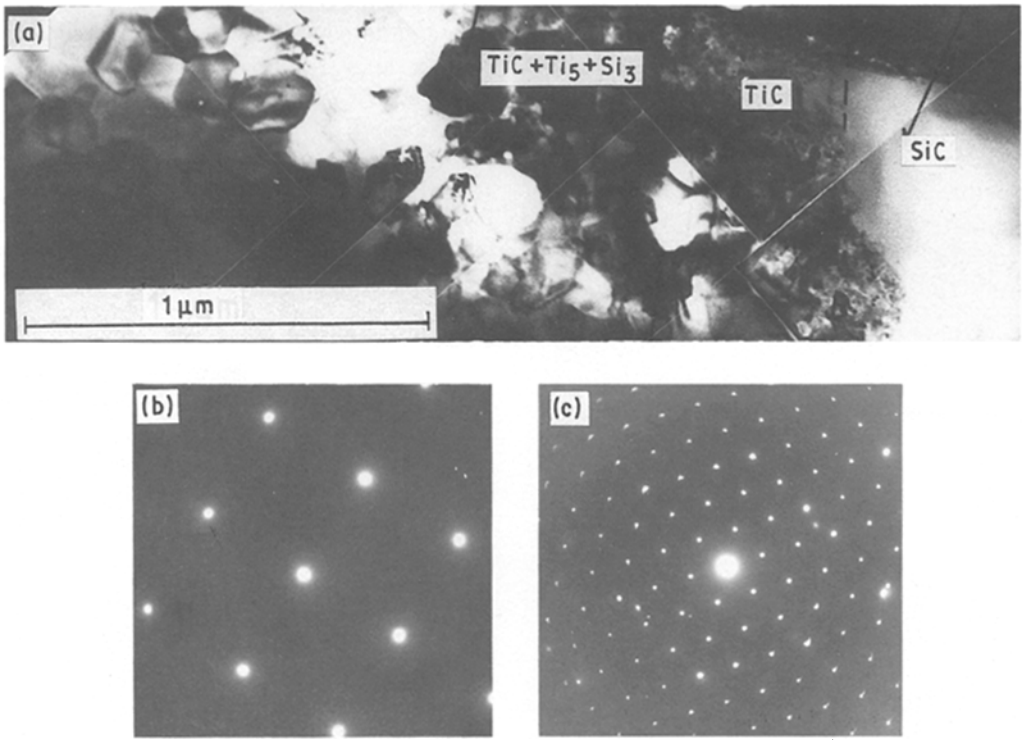

Figure 11 After 900° C, 100 h. (a) Montage revealing the gradation in grain size; (b) single crystal spot pattern of TiC [0 0 1] zone axis; (c) Ti_5Si_3 [0 0 0 1] zone axis.

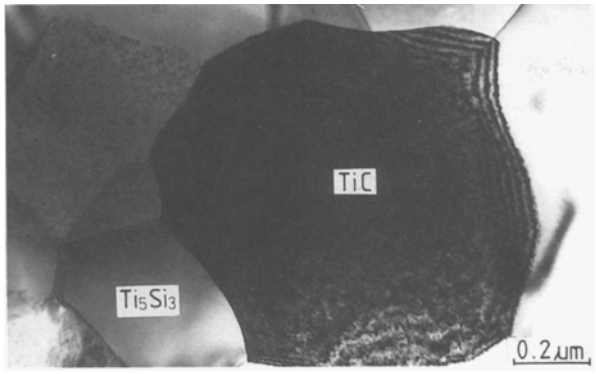

Figure 12 Electron microstructure of TiC (mottled grain) and Ti_5Si_3 (featureless grain).

earlier. Formation of this amorphous layer may be promoted by the oxygen impurities present in SiC. It is well-known that an amorphous (vitreous) layer has an enhanced diffusion rate. The composition of the amorphous layer may be about Ti(C, Si, O). It is logical to assume that TiC nucleates and precipitates from the amorphous phase. This could explain the silicon impurity in the TiC crystals, as observed.

Lastly a comment may be made on the extra reflections observed in the diffraction patterns from the large grains of TiC in the binary zone. It is possible that the carbides in such grains are not stoichiometric, and hence correspond to the composition TiC_{1-x}.

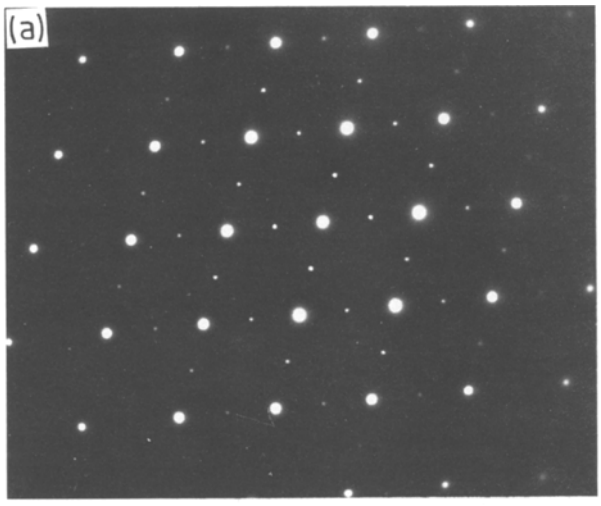

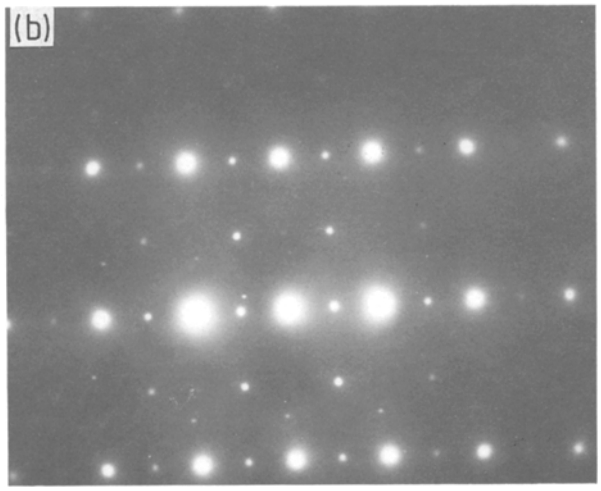

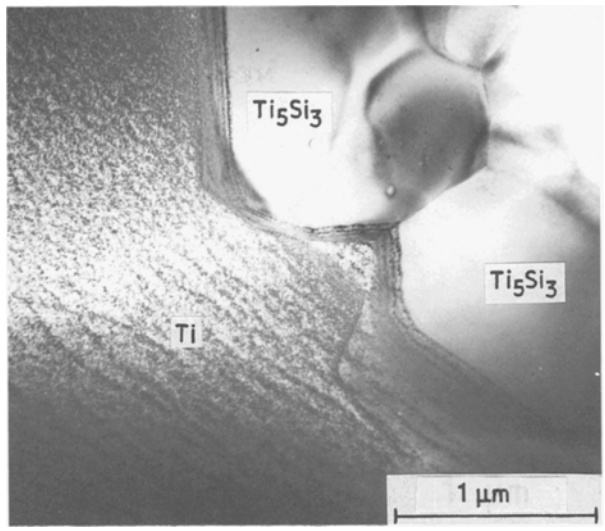

Figure 14 Microstructure showing Ti_5Si_3 adjoining titanium.

Ordered vacancies are possible with such deviations from stoichiometry and the extra reflections are probably due to the resulting complicated structure which has to be further analysed.

5. Conclusions

The thin layer next to SiC is made up primarily of fine grains of TiC with Ti_5Si_3 as a minority phase and the occasional presence of Ti_3SiC_2. The phase in contact with SiC is TiC, possibly containing some silicon as impurity. The diffusion mechanism and the sequence of microstructure formation closely resembles that proposed earlier by Ratliff and Powell [9]. The titanium carbide phase encountered in the binary zone is most likely non-stoichiometric and has a complex structure.

References

1. P. MARTINEAU *et al.*, *J. Mater. Sci.* **19** (1984) 2749.
2. E. P. ZIRONI and H. POPPA, *ibid.* **16** (1981) 3115.
3. H. J. DUDEK, R. LEUCHT and G. ZIEGLER, in Proceedings of the 15th International Conference on Titanium, Vol. III (DGM, Munich, 1984) p. 1773.

Figure 13 Additional reflections at one-half distance of the fcc TiC diffraction patterns. (a) [1 1 0] zone axis; (b) [1 1 2] zone axis; (c) [0 0 1] zone axis.

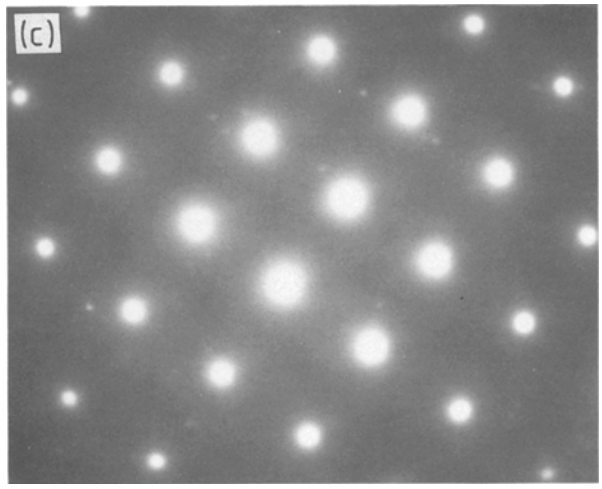

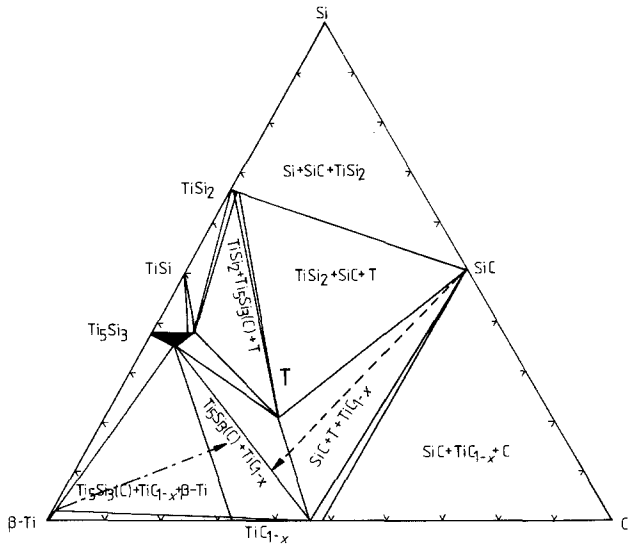

Figure 15 Ti–Si–C ternary phase diagram, 1200° C section according to Brukle [14] on which is superimposed the path followed by the reaction of titanium with SiC. (–·–·–·–), Path followed by metal reaction zone; (– – –), path followed by fine layer zone.

4. J. A. SNIDE, Compatibility of vapour-deposited B, SiC, and TiB filaments with several titanium matrixes, AFML-TR-67-354, 1968 (US Department of Commerce, Springfield, Virginia, Ohio).
5. J. THEOBAULT *et al.*, *J. Less-Common Metal* **47** (1976) 221.
6. V. B. RAO, C. R. HOUSKA and J. UNNAM, in Proceedings of a Conference on New Developments and Applications in Composites, St. Louis, October 16–17 (1978) (TMS-AIME, St. Louis, Missouri, 1978) p. 347.
7. K. P. STAUDHAMMER, L. E. MURR and C. MARINOFF, *Microstructures* **3**(4) (1972) 17.
8. M. J. KLEIN, Compatibility Studies for Variable Titanium Matrix Composites, AFML-TR-69-242 (US Department of Commerce, Springfield, Virginia, 1969).
9. J. L. RATLIFF and G. W. POWELL, Research on Diffusion in Multiphase Systems, and Reaction Diffusion in Ti/SiC and Ti6Al4V/SiC systems, AFML-TR-70-42 (US Department of Commerce, Springfield, Virginia, 1970) p. 57.
10. A. G. METCALFE (ed) in "Metal Matrix Composite" Vol. 1 (Academic, New York, 1974) p. 67.
11. R. WARREN and C. H. ANDERSSON, *Composites* **15** (1984) 101.
12. S. MOROZUMI, M. ENDO and M. KIKUCHI, *J. Mater. Sci.* **20** (1985) 3976.
13. S. K. CHOI, L. FROYEN and M. J. BRABERS, in Proceedings of the International Conference on Joining Ceramics, Glass and Metal. Bad Nauheim (FRG), 1989, edited by W. Kraft (DGM, Munich, 1989) p. 297.
14. C. E. BRUKL, in "Ternary Phase Equilibria in Transition Metal–Boron–Carbon–Silicon Systems", Part II, Vol. VII, AFML-TR-65-2 (US Department of Commerce, Springfield, Virginia, 1965) p. 425.
15. A. D. SMIGELSKAS and E. O. KIRKENDALL, *Trans. Met. Soc. AIME* **142** (1947) 171.

Received 7 March
and accepted 7 June 1989